# Driven kinks in discrete chains: Phonon damping

C. Cattuto,[1,2] G. Costantini,[3] T. Guidi,[3] and F. Marchesoni[2,3]
[1]*Dipartimento di Fisica, Università di Perugia, I-06123 Perugia, Italy*
[2]*Michigan Center for Theoretical Physics, University of Michigan, Ann Arbor, Michigan 48109-1120*
[3]*Istituto Nazionale di Fisica della Materia, Università di Camerino, I-62032 Camerino, Italy*
(Received 10 August 2000; published 27 March 2001)

Phonon radiation is shown numerically to damp the motion of a relativistically driven $\phi^4$ soliton, even in the extremely weak discreteness limit. At higher discreteness, the soliton mobility is characterized by a discontinuous dependence on the driving force; jumps are related to phonon and breather-radiation thresholds. Moreover, the speed of a *frictionless* soliton cannot be lowered below a certain threshold value, or else it might get trapped between two adjacent chain sites.

DOI: 10.1103/PhysRevE.63.046611 PACS number(s): 63.20.−e, 05.45.Yv, 11.27.+d

## I. INTRODUCTION

A variety of physical systems have been modeled in terms of an elastic string diffusing on a periodic substrate, remarkable examples being lattice dislocations, magnetic flux lines in type-II superconductors, triple lines on wetting surfaces, magnetic spin chains, etc. [1]. All these string models belong to the category of soliton-bearing theories, where string transport results from the *lateral* diffusion of single solitons (kinks or antikinks) connecting two adjacent substrate valleys. Propagation of solitons in a viscous medium is by now a fairly well-understood problem in the continuum limit [2–6]. However, with a closer look, all the above-mentioned physical systems imply a certain degree of *discreteness*, stemming from the atomistic structure of the solid phase (i.e., of the string itself and/or of its environment) [6,7].

There is one more reason for investigating the effects of discreteness: Simulation algorithms necessarily replace a continuous string $\phi(x,t)$ with a discrete chain $\{\phi_i(t)\}$, by coarse graining the spatial coordinate $x$ as $i\Delta x$ with $i=1,\ldots,N$. At variance with the problem of modeling an intrinsically discrete system, here discreteness is regarded rather as an unavoidable numerical nuisance one must account for, in order to interpret correctly the simulation outcome. In one dimension, algorithmic discreteness is measured by the ratio $\epsilon=\Delta x/d$, where $\Delta x$ is the spatial quantization step and $d$ denotes the spatial extension of the single soliton (that is, the intrinsic elastic string length); supposedly, on taking $d$ large, discreteness corrections would vanish. This general rule proved correct in the overdamped limit $\alpha_0 \gg \omega_0$, where all speeds involved are much smaller than the string-limiting speed $c_0$ and all relevant relaxation mechanisms occur at rates of the order of the viscous constant $\alpha_0$, that is, much larger than the intrinsic string frequency $\omega_0$. However, in the opposite limit, $\alpha_0 \ll \omega_0$, solitons behave like ultrarelativistic particles with average speed $u$ close to $c_0$. The effective soliton size, $d(u)=d\sqrt{1-u^2/c_0^2}$, then shrinks to values smaller than the string length (note that $d \equiv c_0/\omega_0$) and possibly even shorter than the chain constant $\Delta x$; as a result, regardless of the ratio $\Delta x/d$, the driven soliton eventually perceives the discrete structure of its support and starts radiating phonons [7–11].

Phonon radiation by a discrete soliton has a simple qualitative explanation: As a soliton moves between two adjacent chain sites, its shape gets modulated periodically in time with a certain angular frequency $\omega_S$. Moreover, the phonon spectrum in the presence of the soliton is characterized by a sinusoidal band with the dispersion relation $\omega(i)^2=\omega_0^2[1+(4/\epsilon^2)\sin^2(\pi i/2N)]$. If $\omega_S > \omega_0$, the soliton modulation couples directly with one or more phonon modes; radiation takes place with an intensity that increases with the chain discreteness. If $\omega_S < \omega_0$, a less effective soliton-phonon coupling occurs through a parametric resonance mechanism involving higher harmonics, i.e., $n\omega_S = m\omega_0$ with $n^2+m^2 > 2$. The ensuing *phonon damping* has been investigated numerically for a *frictionless* soliton (i) coming to a halt along a strongly discrete chain [8,9] and (ii) oscillating between two chain sites [11]. In both cases, bursts of resonant phonon radiation have been reported [12]. Phonon damping has been analyzed also under stationary conditions [13], where an underdamped, continuous, one-soliton bearing string is maintained in thermal equilibrium. Due to the coupling with the phonon bath, the soliton undergoes Brownian motion with the frequency-dependent damping constant $\alpha(\omega)=\alpha_0 - i\alpha_1(\omega/\omega_0)+\alpha_2(\omega/\omega_0)^2+\cdots$, where $\alpha_0$ is the bare string-damping constant.

In this preliminary report, we investigate the stationary propagation of a driven soliton along a discrete $\phi^4$ chain paying particular attention to the effects of phonon damping. The soliton mobility curves are shown to exhibit sequences of discontinuous jumps that cannot be interpreted in term of phonon radiation resonances alone. We identify positively a phonon-assisted pinning transition and the occurrence of discrete breather radiation.

Most of the results reported here are likely to apply to the sine-Gordon (SG) chain as well. We focused our study on the $\phi^4$ soliton because (a) no coherent depinning of the $\phi^4$ chain from the substrate may take place at variance with the SG chain [16,17]; (b) no multikink solutions are allowed that, unlike the SG case, may be less subjected to phonon damping than the relevant single kink solution [8]; (c) the existence of a continuum $\phi^4$ soliton shape mode, with frequency smaller than $\omega_0$ [2], is a minor inconvenience at $\epsilon > 0$, where internal modes branch off the discrete phonon band, even in the SG case [14].

 

## II. PHONON RADIATION

We simulated [15] a *one-soliton* bearing $\phi^4$ chain

$$\ddot{\phi}_i - c_0^2 \Delta_2 \phi_i + V'[\phi_i] = F - \alpha_0 \dot{\phi}_i + \zeta_i(t), \tag{1}$$

with $i=1,2,\ldots,N$, where $\Delta x=1$, $\Delta_2 \phi_i = \phi_{i+1} + \phi_{i-1} - 2\phi_i$, $\zeta_i(t)$ denotes local Gaussian noise sources with $\langle \zeta_i(t) \rangle = 0$ and $\langle \zeta_i(t) \zeta_j(0) \rangle = 2\alpha_0 kT \delta_{ij} \delta(t)$, and $V[\phi]$ denotes the on-site potential $(\omega_0^2/8)(\phi^2-1)^2$. The chain $\{\phi_i\}$ is a free-end chain ($\phi_0=\phi_1, \phi_{N+1}=\phi_N$) with $\phi_1 \simeq \mp 1$ and $\phi_N \simeq \pm 1$ for a kink ($\phi_+$) or an antikink ($\phi_-$), respectively, and long enough for the diffusing soliton not to experience boundary forces. The viscous term $-\alpha_0 \dot{\phi}_i$ and the noise sources $\zeta_i(t)$ guarantee thermalization of the chain at temperature $T$, while a positive constant force $F$ drives $\phi_+$ to the left and $\phi_-$ to the right.

The diffusion of a single soliton along a fluctuating chain is well described (apart from inessential terms) by the relativistic Langevin equation (LE) [2–5]

$$\dot{p} = -\alpha p - V'_{\rm PN}(X) \mp 2F + \xi(t), \tag{2}$$

where $\xi(t)$ is a stationary Gaussian noise with zero mean and autocorrelation function $\langle \xi(t)\xi(0) \rangle = 2\alpha M_l kT \delta(t)$, $M_l \simeq M_0 = 2/3d$ approximates the average discrete (anti)kink mass [18], and $p(u) = M_0 u / \sqrt{1-u^2/c_0^2}$ can be regarded as the momentum of a relativistic soliton with center-of-mass coordinate $X$. Discreteness breaks the $\phi_\pm$ translational invariance by generating a periodic Peierls-Nabarro (PN) potential $V_{\rm PN}(X)$ [6] with constant $\Delta X = \Delta x = 1$; within the accuracy of our numerics [18], $V_{\rm PN}$ is well described by the cosine potential

$$V_{\rm PN}(X) = \frac{k_{\rm PN}}{4\pi^2}[1+\cos(2\pi X)], \tag{3}$$

whose amplitude diverges exponentially with $\epsilon$ [7,10,11].

The stochastic process $X(t)$ was sampled as follows: At regular time intervals $T_X$ (typically $T_X=10$), copies of the chain configuration were recorded and then fed through a filtering routine that makes the chain evolve further in time, at zero temperature and a much larger chain damping constant, $\alpha_0 \gg \omega_0$; as a result, the (anti)kink gets frozen almost instantaneously between two adjacent chain sites. The ensuing quantization (with unit step) of the sampled soliton trajectory, $X_n = X(nT_X)$, has no bearing on the statistics of our simulations, provided that the displacements measured are conveniently long and $T_X$ is chosen to be shorter than any relevant time scale in the problem (but much larger than the freezing time $\alpha_0^{-1}$). From the time dependence of $X(t)$, one then determines the kinetic variables $u(t)$ and $p(t)$.

In order to characterize the soliton damping constant $\alpha$ in Eq. (2) we plotted the stationary (average) soliton momentum $p(F)$ versus the driving force $F$ in the *noiseless* case $T \equiv 0$, for different values of the discreteness parameter $\epsilon$ (Fig. 1) and of the string damping constant $\alpha_0$ (Fig. 2). Our results can be summarized as follows. (i) $p(F)$ is *finite* for any value of $\epsilon$ and, more remarkably, even at $\alpha_0=0$. Note

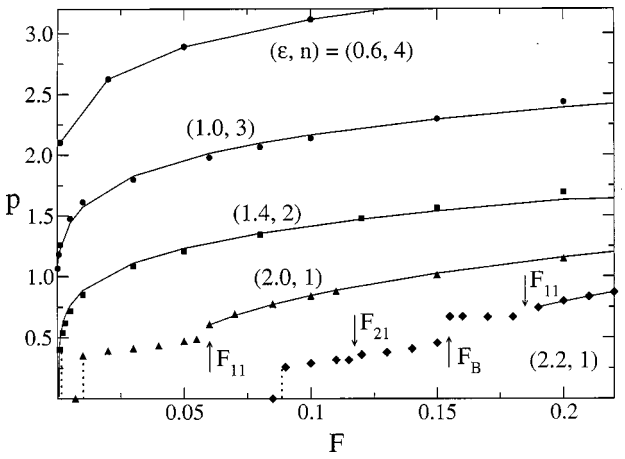


FIG. 1. Stationary soliton momentum (absolute value) $p(F)$ versus $F$ for $\alpha_0=0$, $T=0$, and different values of $\epsilon$ (for convenience $\omega_0$ was kept constant, $\omega_0^2=8$). A stationary value of $p(t)$ corresponds to the asymptotic behavior of the soliton trajectory, $X(t) \propto t$. Jumps due to phonon coupling, $F_{nm}$, and breather radiation, $F_B$, are marked by vertical arrows; the pinning thresholds $F_1$ are represented by dotted lines. The curve branches with $p > p_0$ have been fitted by means of the heuristic law $\sqrt[2n+1]{2(F-F_0)/\alpha_n}$, where $n$ has been set *ad hoc* to increase with decreasing $\epsilon$ (see labels). These curves do not depend on the initial conditions, provided that the chain evolves eventually towards a stationary running state.

that for the smallest $\epsilon$ value reported in Fig. 1, the static soliton parameters are almost indistinguishable from the continuum limit (e.g., $M_l$ and $M_0$ coincide within three significant digits [18]). (ii) At variance with the overdamped limit, $p(F)$ is never proportional to $F$, not even above the depinning threshold $F_3 = k_{\rm PN}/4\pi$ (see Fig. 2); the curves $p(F)$ get flatter and flatter for $\epsilon$ tending to zero, as illustrated by the

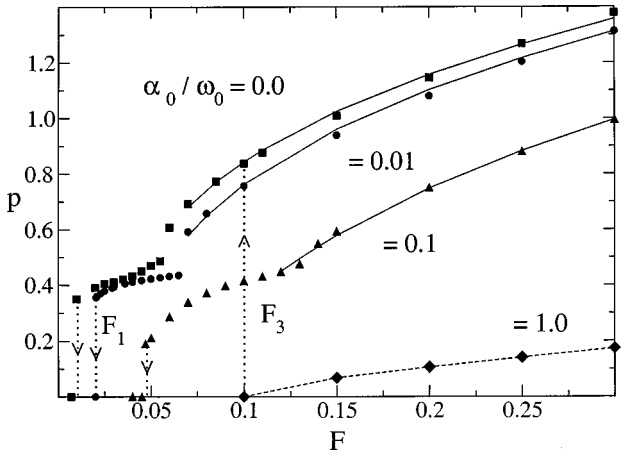


FIG. 2. $p(F)$ versus $F$ for $\epsilon=2.0$, $T=0$, $\omega_0^2=8$, and increasing values of $\alpha_0$. The pinning, $F_1$, and depinning thresholds, $F_3$, of each curve are marked by downward and upward oriented dotted lines, respectively. The solid fitting curves have been drawn by solving Eq. (5), after truncation at $n=1$: on raising $\alpha_0$, the fitted parameter values are $(\alpha_1, F_0) = (0.207, 0.038)$, $(0.207, 0.038)$, and $(0.207, 0.049)$. The dashed fitting curve for the overdamped case $\alpha_0/\omega_0 = 1.0$, see Ref. [18], is reported for the sake of comparison.

heuristic fits of Fig. 1. (iii) All the curves plotted in Figs. 1 and 2 exhibit an upper branch that starts out discontinuously at $p_0 \equiv p(u_0)$ with $u_0 = \omega_0/2\pi < c_0$. In fact, solitons with average speed $u > u_0$ get modulated in shape with frequency $\omega_S$ larger than $\omega_0$, i.e., they exchange energy directly with the phonon modes [8]. (iv) Such a property is robust towards the string viscosity, as the gap at $p = p_0$ smooths out into a cusp only for $\alpha_0/\omega > 0.1$. (v) For $p < p_0$ and relatively strong discreteness, the $p(F)$ curves show a number of steplike discontinuities, or jumps, that end at a minimum threshold value $F_1$ of the driving force, below which no stable running state could be observed, despite our initial condition search [19] and at odds with an earlier simulation by Peyrard and Kruskal [8]. Therefore, we conclude that, as an effect of discreteness, a sharp *pinning transition* takes place at $F = F_1$. In the noiseless limit, the soliton response to the external drive in the interval $F_1 \leqslant F \leqslant F_3$ displays a hysteretic dependence on the initial conditions [16,17]; therefore, the mobility data reported in Figs. 1 and 2 refer to the initial string configurations that sustain stationary soliton running states [19].

### III. PHONON DAMPING

We interpret now the outcome of our simulation. We focus first on the ultrafast solitons with $p > p_0$. As anticipated above, due to the Lorentz contraction, accelerated relativistic solitons end up ''interacting'' with the chain sites and thus radiating phonons. In view of the formal analysis of Ref. [13], we assume that the ensuing (average) phonon damping can be reproduced quite generally by the nonlinear viscous term

$$\alpha p \rightarrow \alpha(p) p = \alpha_0 p + \alpha_1 p^3 + \cdots + \alpha_n p^{2n+1} + \cdots, \quad (4)$$

where $\alpha_0$ is the bare string damping constant and the remaining coefficients $\alpha_n$ can be fitted, at least in principle, from the simulation data. A rough estimate of the stationary $p$ value at zero temperature follows immediately from the ''mean-field'' equation

$$\dot{p} = 0 = -\alpha_0 p - \alpha_1 p^3 - \cdots - \alpha_n p^{2n+1} - \cdots \mp 2(F - F_0), \quad (5)$$

where the additional tilt $F_0 = F_0(\alpha_0, \epsilon)$ mimics the average effect of the PN potential (3) [20]. In the regime of strong discreteness, say $\epsilon \geqslant 2$, Eq. (5) may be safely truncated at $n = 1$. In the frictionless case, $\alpha_0 = 0$, one obtains the two-parameter fitting curve $p(F) = \sqrt[3]{2(F - F_0)/\alpha_1}$, whereas for *finite* but small values of the string damping constant, $\alpha_0/\omega_0 < 0.1$, the stationary soliton momentum coincides with the real root of the cubic equation (5) with $n = 1$. This interpretation of our results is confirmed quantitatively in Fig. 2, where, in the underdamped limit, the fitted parameters $\alpha_1$ and $F_0$ appear not to depend on $\alpha_0$. Our fits show that even for $\alpha_0/\omega_0 = 0.1$, phonon damping is still appreciable and decoupled from the string damping (i.e., $\alpha_1$ is independent of $\alpha_0$); on the contrary, $F_0$ grows with $\alpha_0$, as suggested in Ref. [20]. On lowering $\epsilon$, one expects that the coefficients $\alpha_n$, with $n > 1$, fall off exponentially [6,7,10]; as a result, the stationary solution (5) for $p$ would be dominated by increasingly higher powers, $n$, of the phenomenological expansion (4) (see the fits of Fig. 1).

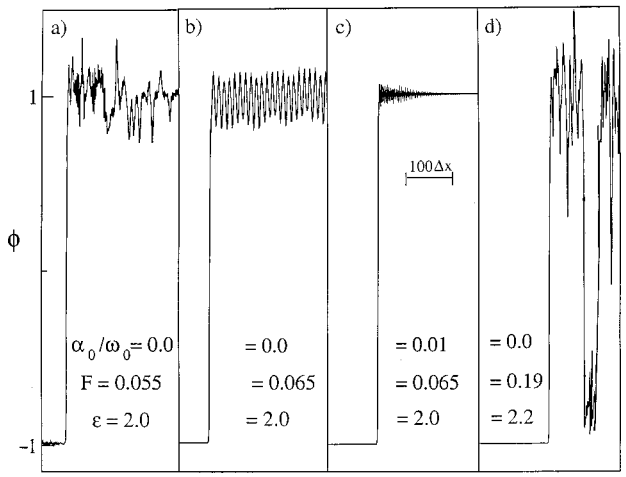


FIG. 3. Phonon radiation by a propagating kink for different values of $\alpha_0$, $F$, and $\epsilon$ and the same $x$ scale (see labels). All snapshots refer to stationary states from Fig. 2 and were taken after $10^6$, or more, integration steps with $\Delta t = 10^{-3}$.

Phonon radiation is responsible for the renormalization of the viscous term (4). Snapshots of a propagating $\phi^4$ kink are displayed in Fig. 3 for different values of $\epsilon$, $F$, and $\alpha_0$. Each kink is followed by a phonon trail, its amplitude being much larger for $p > p_0$ (direct soliton-phonon coupling) than for $p < p_0$ [resonant coupling, Figs. 3(a) and 3(b)], and quenched by the string damping over a characteristic attenuation length $u/\alpha_0$ [Fig. 3(c)]. While phonon radiation from traveling discrete solitons has been reported in [8–11], and even earlier [21], our simulation revealed that the phonon tail points opposite to the applied drive, *independently* of the actual direction of kink propagation. We accelerated a frictionless kink to the left [like in Fig. 3(a)] by applying a constant force $F$; upon reflection, the kink bounces to the right against the driving force (not displayed). Quite surprisingly (see Refs. [8,22]), the phonon tail looks now to build up in the forward direction [a chain snapshot would be almost indistinguishable from Fig. 3(a)].

We address now the discontinuous jumps of the soliton mobility for $p < p_0$ and *zero temperature*, where the phenomenon of resonant phonon radiation is expected to play a key role [8,11]. The pinning step at $F = F_1(\alpha_0, \epsilon)$ is a very robust feature, as it persists even for values of the string damping constant where the $p = p_0$ jump disappears (see Fig. 2). Although the threshold $F_1$ could be determined with extremely high precision, we could not relate the underlying pinning mechanism to any abrupt change in the soliton dynamics, such as the emission of phonon bursts [11], the onset of internal oscillations [23], or the like: The soliton simply stops propagating and its kinetic energy is gradually given away in the form of symmetrically dispersing string oscillations.

The remaining jumps, more numerous upon raising $\epsilon$ above 1, fall into two categories. (i) *Soliton-phonon* coupling, $n\omega_S = m\omega_0$ [8,11], with relevant resonance thresholds

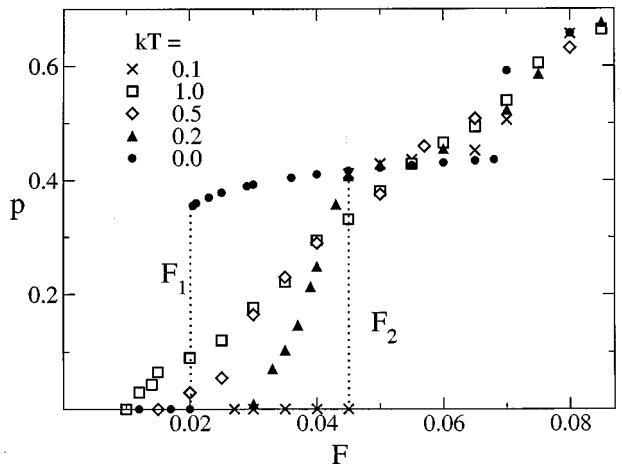


FIG. 4. Stationary soliton momentum (absolute value) $p(F)$ versus $F$ for $\alpha_0/\omega_0=0.01$, $\omega_0^2=8$, $\epsilon=2$, and different values of $kT$ (in units of $k_{\rm PN}/4\pi^2$). The pinning thresholds $F_1$ and $F_2$ (see the text) are marked by dotted lines. Simulation parameters: integration step, $\Delta t=10^{-3}$; run length, $5\times10^6$ integration steps. Note that for the smallest $kT$ value simulated, a more accurate definition of the (continuous) transition step would require exceedingly long computer runs.

at $F_{nm}$. The ubiquitous threshold $F_{11}$ corresponds to the $p=p_0$ jump, whereas a threshold $F_{21}$ can be recognized positively in Fig. 1 only for the strongest discreteness case simulated. Higher-order steps with $m>1$ and $n>2$ could not be safely identified, due to the presence of the pinning transition; even at higher $\epsilon$ values (not shown), the expected jump size is too small to be statistically appreciable. (ii) *Soliton-breather* coupling. To the best of our knowledge, this is the first instance where a relativistic kink is shown to radiate a discrete doublet [or breather, see Fig. 3(d)]. A discrete chain is known to bear bound kink-antikink states [24] with discrete energy levels in the range $(0,2E_0)$, with $E_0=M_0c_0^2$. Such structures are unstable under the action of the radiating soliton [25], not to mention the external drive; breather emission implies a high activation threshold, which may only be overcome in the regime of strong discreteness.

Finally, in Fig. 4 we assessed the stability of the pinning mechanism in the presence of thermal fluctuations. At finite temperature (i.e., for $kT$ of the order of $k_{\rm PN}/4\pi^2$ or smaller), the pinning jump at $F=F_1$ is replaced by an abrupt surge of the $p(F)$ curve from zero up to its noiseless value, while the hysteretic dependence on the initial string configuration is suppressed. On decreasing the string temperature, the pinning jump approaches, and gets more and more confined around a new $T=0+$threshold $F_2(\alpha_0,\epsilon)$. The thresholds $F_1$ and $F_2$ are not immediately related to the underlying kink PN potential [10], nor to long-range string interactions as in Ref. [26]: *Soliton pinning is caused here primarily by discreteness-induced phonon radiation*. At higher temperatures, the pinning transition smooths out, as the role of resonant phonon damping gets less and less appreciable. On the contrary, the stationary momentum of ultrafast solitons depends marginally on the string temperature, thus suggesting that for $p>p_0$ direct phonon damping retains a prominent role even at finite temperature.

We acknowledge partial support from the Michigan Center for Theoretical Physics (MCTP), University of Michigan (Ann Arbor).

[1] Most of these models are outlined in M. Remoissenet, *Waves Called Solitons* (Springer, Berlin, 1994); R. K. Dodd, J. C. Eilbeck, J. D. Gibbon, and H. C. Morries, *Soliton and Nonlinear Equations* (Academic Press, London, 1982); J. P. Hirth and J. Lothe, *Theory of Dislocations* (Wiley, New York, 1982).

[2] J. F. Currie *et al.*, Phys. Rev. B **22**, 477 (1980).

[3] R. Boesch and C. R. Willis, Phys. Rev. B **39**, 361 (1989), and references therein.

[4] F. Marchesoni, Phys. Lett. A **115**, 29 (1986).

[5] D. W. McLaughlin and A. C. Scott, Phys. Rev. A **18**, 1652 (1978); M. Salerno, E. Joergensen, and L. R. Samuelsen, Phys. Rev. B **30**, 2035 (1984).

[6] For a review, see O. M. Braun and Yu. S. Kivshar, Phys. Rep. **306**, 1 (1998).

[7] J. F. Currie *et al.*, Phys. Rev. B **15**, 5567 (1977).

[8] M. Peyrard and D. Kruskal, Physica D **14**, 88 (1984). Note that we simulated longer chains, typically $N=5000$, with much shorter integration steps, $\Delta t=10^{-4}$–$10^{-3}$, and for longer runs (up to $10^4$ time units).

[9] M. Peyrard and M. Remoissenet, Phys. Rev. B **26**, 2886 (1982).

[10] C. Kunz and J. A. Combs, Phys. Rev. B **31**, 527 (1985); J. A. Combs and S. Yip, *ibid.* **28**, 6873 (1983).

[11] R. Boesch, C. R. Willis, and M. El-Batanouny, Phys. Rev. B **40**, 2284 (1989).

[12] For a trapped kink, $\omega_S$ is well approximated by $\omega_{\rm PN}=\sqrt{k_{\rm PN}/M_0}$ and increases slightly by damping the oscillation amplitude. As $\omega_S<\omega_0$ [11], phonon radiation is always of the resonant type $n^2+m^2>2$.

[13] F. Marchesoni and C. R. Willis, Europhys. Lett. **12**, 491 (1990).

[14] R. Boesch and C. R. Willis, Phys. Rev. B **42**, 2290 (1990).

[15] Our simulation code is a framework based on Numerical Python and custom C libraries. Time integration is performed by means of a modified Mil'shtein algorithm, at finite $T$, and a standard fourth-order Runge Kutta for $T=0$. For further details, see also F. Marchesoni, C. Cattuto, and G. Costantini, Phys. Rev. B **57**, 7930 (1998).

[16] C. Cattuto and F. Marchesoni, Phys. Rev. Lett. **79**, 5070 (1997).

[17] O. M. Braun, A. R. Bishop, and J. Röder, Phys. Rev. Lett. **79**, 3692 (1997); O. M. Braun *et al.*, *ibid.* **78**, 1295 (1997).

[18] An accurate determination of the discrete soliton mass $M_l$ is reported by T. Guidi, C. Cattuto, and F. Marchesoni (unpublished).

[19] For $p>p_0$, it suffices to start with a steplike chain configuration, which reproduces a kink centered somewhere along the chain. As the chain arranges itself towards the profile of a stable discrete kink, it radiates a phonon burst that, combined with the tilt $F$, pushes the kink over the lower PN barrier, thus activating its translational motion. For $p<p_0$, the soliton stationary state is more sensitive to the string initial conditions. In order to check the existence of the $p(F)$ jumps, we sampled the relevant chain phase space by means of a Monte Carlo algorithm, searching for all movable initial configurations.

[20] H. Risken, *The Fokker-Planck Equation* (Springer, Berlin, 1984), Chap. 11.

[21] A. D. Brailsford, Phys. Rev. **122**, 778 (1961).

[22] Y. Ishimori and T. Munakata, J. Phys. Soc. Jpn. **51**, 3367 (1982).

[23] Y. S. Kivshar *et al.*, Phys. Rev. Lett. **80**, 5032 (1998); P. G. Kevrekidis and C. K. R. T. Jones, Phys. Rev. E **61**, 3114 (2000).

[24] R. Boesch and M. Peyrard, Phys. Rev. B **43**, 8491 (1991).

[25] S. V. Dimitriev *et al.*, Phys. Rev. E **61**, 5880 (2000).

[26] S. F. Mingaleev *et al.*, Phys. Rev. E **61**, 4454 (2000).